Combined Multiphoton and Optical Coherence Microscopy

Shuo Tang, Tatiana B. Krasieva , Zhongping Chen, and Bruce J. Tromberg

Laser Microbeam and Medical Program, Beckman Laser Institute
University of California, Irvine, CA 92612

ABSTRACT

Multiphoton microscopy (MPM) and optical coherence tomography (OCT) are two important techniques for non-invasive and high-resolution imaging of highly scattering biomedical tissues. MPM and OCT provide complementary information about tissues as the detected signals originate from different substances and mechanisms. Combining MPM and OCT can simultaneously provide rich functionality and morphology information about biomedical tissues. We report a novel system which combines multiphoton and optical coherence microscopy. A femtosecond Ti:Sapphire laser is used as the light source which has a pulse width of 10 fs and a spectral bandwidth of 100 nm. The ultrafast Ti:Sapphire laser provides the short pulse and the broad bandwidth required by high-resolution MPM and OCT, respectively. By matching the resolution and the imaging volume of MPM and OCT, we achieved co-registration between the MPM and OCT images. Dispersion compensation is critical in this MPM/OCT system and its effect is discussed. Representative images of co-registered MPM/OCT are presented.

Keywords: Multiphoton microscopy, optical coherence tomography, second harmonic generation, femtosecond laser, dispersion compensation

1. INTRODUCTION

Multiphoton microscopy (MPM)[1] and optical coherence tomography (OCT)[2] are two important techniques for non-invasive and high-resolution imaging of highly scattering biomedical tissues. MPM and OCT provide complementary information about tissues as the detected signals originate from different substances and mechanisms in the tissues. MPM includes both two-photon excited fluorescence (TPEF) and second harmonic generation (SHG). TPEF can be excited from either endogenous or exogenous fluorophores, which indicates the functionality of cells. Strong SHG signal has been generated by extracellular matrix protein collagen. OCT detects backscattered light from the inhomogeneity of the tissues. Therefore, combining MPM and OCT can simultaneously provide rich functionality and morphology information about biomedical tissues.

Previous research has studied wound healing after laser ablation using both MPM and OCT technologies.[3] The images are taken from separate MPM and OCT systems. With relatively low resolution, the OCT images can cover a large area to locate the injury. High resolution MPM images are then taken to show details about the cellular and extracellular structures of the injured and uninjured areas. With the information from both MPM and OCT, a good understanding of the process of wound healing can be achieved. However, the previous research is done on two separate systems. When the sample is moved from one system to another, it is very difficult to find the exact location where the other system has imaged. Furthermore, the MPM and OCT systems have different resolutions such that it is hard to compare their images directly. Therefore, it will be very useful to have a combined MPM/OCT system on the same platform where high resolution MPM and OCT images can be simultaneously taken from the same sampling area.

Combined MPM/OCT system has been reported before,[4] where a 80 fs Ti:Sapphire laser has been used. The coherence length of such a laser source is only 15 μm. Thus to increase the resolution of the OCT channel, a pinhole is inserted before the OCT detector, which results in significant signal loss. Recently, laser technology has much improved so that a Ti:Sapphire laser with much shorter pulse duration and broader bandwidth is commercially available now. Therefore, high resolution MPM/OCT can be achieved without the need of a pinhole design.

In this manuscript, we report a novel system which combines multiphoton microscopy and optical coherence tomography. An ultrafast Ti:Sapphire laser (Femtolasers, Vienna, Austria) is used as the light source. The laser has a pulse width

Further author information: (Send correspondence to Shuo Tang)
E-mail: stang@laser.bli.uci.edu, Telephone: 1(949)824-4104

Multiphoton Microscopy in the Biomedical Sciences V, edited by Ammasi Periasamy, Peter T. C. So, Proceedings of SPIE Vol. 5700 (SPIE, Bellingham, WA, 2005)
1605-7422/05/$15 · doi: 10.1117/12.591257

of 10 fs and a spectral bandwidth of 100 nm. Thus the coherence length of the light source is calculated to be about 2.8 μm, assuming a Gaussian spectral shape. Therefore, high-resolution MPM and OCT imaging can be achieved with the same ultrafast laser. However, with such a broad bandwidth, pulse broadening and dispersion compensation are critical in this MPM/OCT system, which will be discussed in details in the next sections. Preliminary images of co-registered MPM/OCT will also be presented.

2. SYSTEM DESIGN

The experimental setup of the combined MPM/OCT system is shown in Fig. 1. The femtosecond Ti:Sapphire laser is pumped by a Nd:YVO_4 laser. The laser output from the Ti:Sapphire first passes through a dispersion precompensation unit to compensate the material dispersion from the objective lens and other optics in the beam path. The dispersion precompensation unit consists of a pair of chirped mirrors and a setup of dispersion compensating prism-pair. The amount of dispersion that can be compensated is adjusted by the apex separation between the two compensating prisms. After the dispersion precompensation unit, the laser beam is split by a beam splitter into two branches, one is the sample arm and the other is the OCT reference arm. In the sample arm, the laser beam is raster scanned in an *en-face* mode by two Galvanometer scanners. The scanning laser beam then enters a Zeiss Axioskop microscope and incidents on the sample. In the OCT reference arm, a scanning piezo mirror generates the modulation frequency for OCT detection. In the *en-face* scanning mode, the scanning range of the piezo mirror is set to be very small so that the OCT signal is sampled only on a thin slice. A second prism pair is set up in a configuration of variable material thickness to balance the dispersion between the sample and the reference arms. When ultrashort laser pulses incident on the sample, a variety of signals are generated by the sample and are further detected by multiple channels. In this combined MPM/OCT system, three detection channels can simultaneously detect TPEF, SHG, and OCT signals, respectively. The TPEF and SHG signals are separated by dichroic mirrors and detected by two photon multiplier tubes (PMTs). The back scattered signal goes backward and is sent to a PIN detector where it is mixed with the reflected signal from the reference arm. OCT interference fringes are generated on the PIN detector when the path length of the reference arm matches with that of the sample arm within the coherence length. The envelop of the interference fringes is further recovered by a lock-in amplifier. All the signals from the PMTs and the lock-in amplifier are sent to a computer where images are recorded.

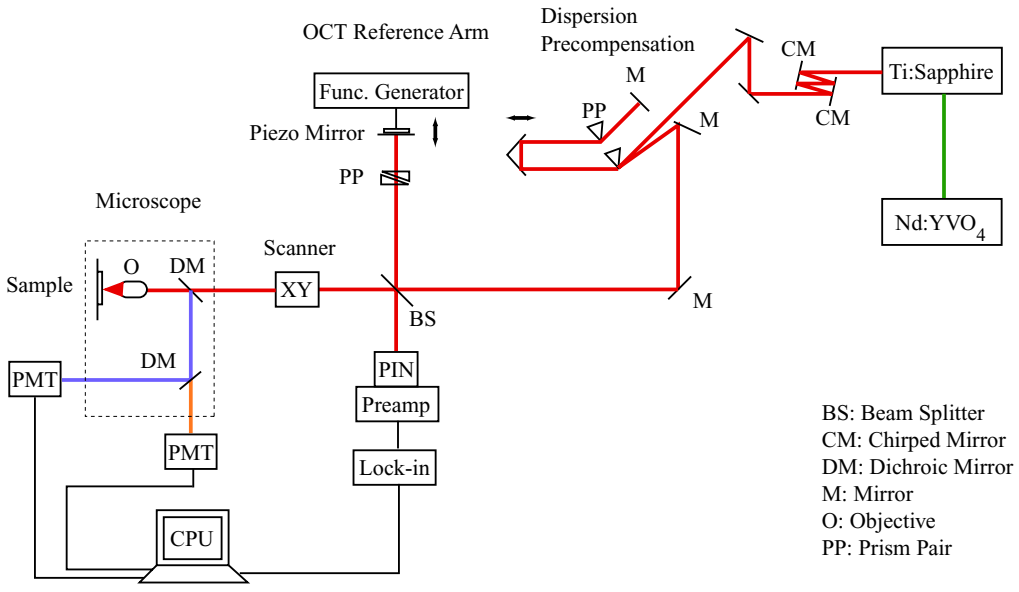

Figure 1. Schematics of the combined MPM/OCT system.

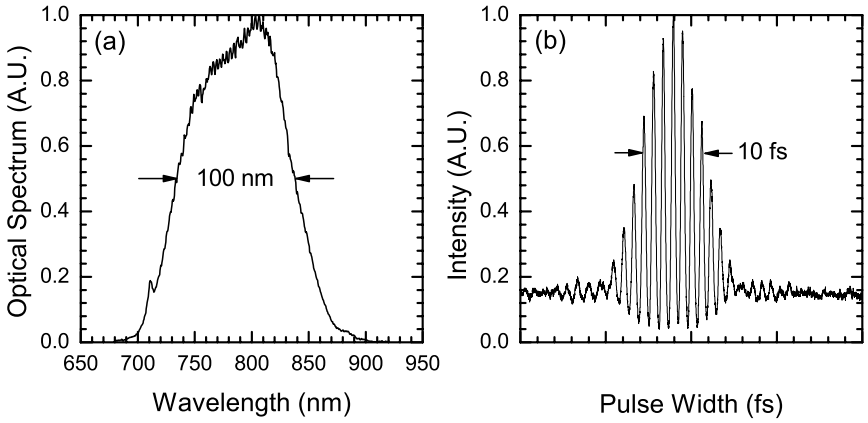

Figure 2. Characteristics of the ultrafast Ti:Sapphire laser. (a) Optical spectrum. (b) Autocorrelation trace.

In the combined MPM/OCT system, it is important to co-register MPM and OCT images, which means to image the same sampling volume in both MPM and OCT. MPM signal is excited from the sampling volume where the laser beam is tightly focused. Therefore, its transverse and axial resolutions are determined by the focal diameter and focal depth of the objective lens, respectively. For OCT signal, its transverse resolution is still determined by the focal diameter of the objective lens. However, its axial resolution is defined by the coherence length of the light source. For an objective lens of 0.9 numerical aperture (N.A.), the focal diameter can be as small as 0.5 μm and the focal depth can be as short as 1.5 μm. Therefore, the sampling volume in MPM is about 1 μm^3. For OCT signal, in order to achieve the same axial resolution, the coherence length of the light source has to be close to 1.5 μm. In our case, we use an ultrafast Ti:Sapphire laser which has a pulse width of 10 fs and a bandwidth of 100 nm. Thus the coherence length is about 2.8 μm assuming a Gaussian spectral shape. Therefore, with the ultrafast Ti:Sapphire laser, the resolution of MPM and OCT can be matched without the need of a pinhole.

The characteristics of the Ti:Sapphire laser is shown in Fig. 2. Fig. 2(a) shows its optical spectrum where the bandwidth is measured to be 100 nm. Fig. 2(b) shows the auto-correlation trace of the laser pulse where its full width at half maximum (FWHM) is measured to be 10 fs. OCT resolution can be measured from the interference fringes when a flat mirror is placed on the sample position. The interference fringes are shown in Fig. 3 where the FWHM is measured to be about 4.8 μm. The reason that the measured OCT resolution is lower than the idea case could be that the spectral shape of the light source is not an ideal Gaussian and the dispersion between the sample and the reference arms may not be completely balanced. Nevertheless, the OCT signal still has a very high resolution which is close to that of MPM.

While the broadband laser source gives the OCT signal high resolution, it also imposes challenges on pulse broadening and dispersion compensation in the system. With a 100 nm bandwidth, the laser pulse gets easily broadened before it reaches the sample. The major dispersive component in the system is the high N.A. objective lens. The group velocity dispersion (GVD) of a Zeiss IR-Achroplan 63X/0.9 water objective is measured to be about 1500 fs^2 value.[5] To compensate those GVD in the system, the dispersion precompensation unit as shown in Fig. 1 is designed. The majority of the GVD is compensated by the prism pair which has an apex separation of about 1.3 m. Chirped mirrors is another candidate for dispersion compensation. In our system, a pair of chirped mirrors are also used which can compensate for up to a few hundred fs^2 GVD. As the efficiency of MPM excitation depends on the concentration of photon flux, under the same average laser power, a shorter pulse tend to be more efficient in exciting MPM signal. We will discuss about this issue in details in the next sections.

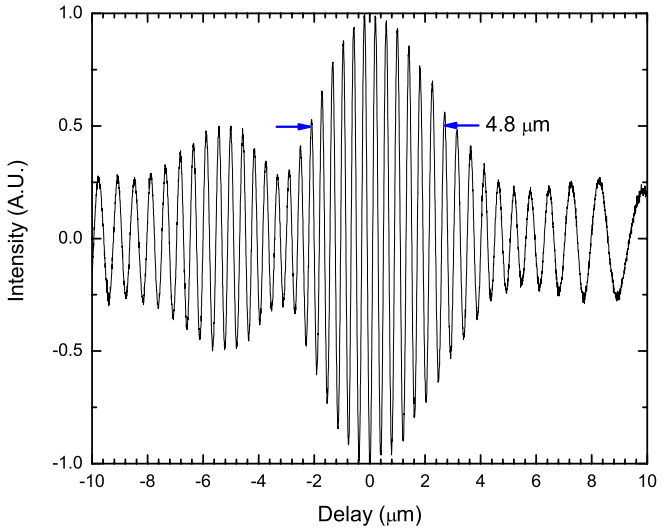

Figure 3. Interference fringes showing OCT resolution.

3. SAMPLE PREPARATION

Fluorescent beads are first imaged by the combined MPM/OCT system. The fluorescent beads are 6 μm in diameter. The beads are first mixed with distilled water. A droplet of such mixture is then put on a glass slide and covered with a cover slip. The slide with fluorescent beads is then imaged with the combined MPM/OCT system. The beads generate very bright fluorescent signal under two-photon excitation at 800 nm. The beads are also very good scattering centers for generating back scattered signals for OCT detection.

Fibroblast cluster is also imaged by the combined MPM/OCT system. Fibroblasts are cultured in nutritious media. They grow into a ball shape of the diameter of about 1.5 mm. The fibroblast cluster is then stained with red dye and mounted in a imaging dish for further imaging. After staining, the nuclei of the fibroblasts are very bright in fluorescence with two-photon excitation at 800 nm. The back scattering OCT signal comes from the inhomogeneous structure of the cells and extracellular structure.

4. RESULTS AND DISCUSSIONS

4.1. MPM EXCITATION AND PULSE DURATION

MPM signal depends quadratically on the excitation intensity. Therefore, MPM signal tends to increase as the excitation pulse duration is reduced with the same average power. However, there is also the effect of saturation and photobleaching. Thus it is very important to study how the MPM signal changes with pulse duration. In our experiment, we can vary the pulse duration by adjusting the amount of compensating dispersion. With a longer apex separation between the dispersion compensating prism pair, a larger amount of positive dispersion is introduced. The laser pulse is at the shortest when the negative material dispersion from the optics is all compensated by the positive dispersion from the prism pair. When the dispersion is under or over compensated, the pulse duration increases. In the experiment, we use fluorescein as the two-photon excitable fluorescent sample. The two-photon excited fluorescence intensity is recorded while the apex separation of the prism pair is changed. Fig. 4 shows the TPEF intensity versus the apex separation. The objective lens is a Zeiss IR-Achroplan 63X/0.9 water objective. As we can see, the intensity of TPEF first increases when the apex separation is increased. Then the TPEF reaches a plateau with fluctuations in the middle. Finally, the TPEF intensity starts to decrease when the apex separation is further increased.

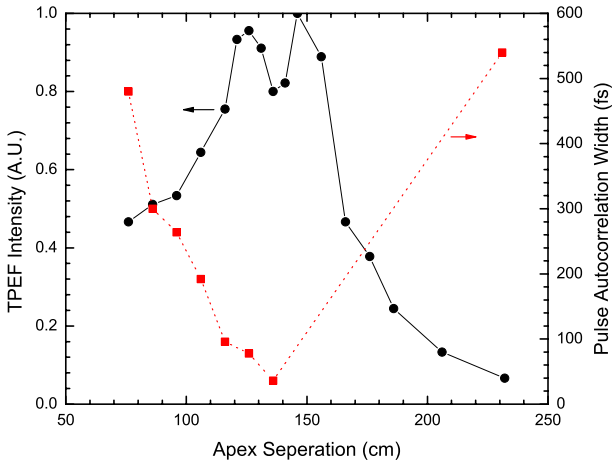

Figure 4. Intensity of TPEF and measured pulse width under different apex separations.

In order to check how the pulse duration changes with the apex separation of the dispersion compensating prism pair, the pulse duration is measured with an auto-correlator. In our setup, the OCT reference arm has the second prism pair to introduce some variable material dispersion. The amount of positive material dispersion is varied by changing the thickness of the material where the beam passes through. Only when the dispersion in the sample arm is the best balanced by the dispersion in the reference arm, we get the highest resolution in the OCT interference fringes. When the dispersion in the sample arm is balanced by that in the reference arm, we can estimate the pulse width under the microscope by measuring the pulse width in the reference arm. Fig. 4 also shows the measured autocorrelation width of the laser pulse measured in the reference arm under different apex separations. As we can see, when the apex separation is at about 1.3 m, the autocorrelation width is the shortest which is about 30 fs. The pulse width increases when the apex separation is shorter or longer than 1.3 m, which indicates that the dispersion is under or over compensated. Comparing the two curves in Fig. 4, we can see that the TPEF intensity is at the maximum when the pulse duration is less than 100 fs. When the pulse duration is longer than 100 fs, the TPEF decreases fast. When the pulse duration is within 100 fs, the TPEF shows a plateau with a dip in the center. This dip is probably caused by the effect of saturation and photobleaching.

For different objective lens, the TPEF intensity changes differently with the pulse duration. Fig. 5 shows the TPEF intensity obtained with a Plan-Neofluar 10X/0.30 objective lens compared with the 63X objective lens, under different apex separations of the prism pair. As we can see, the TPEF intensity peaks at a shorter apex separation in the 10X, which means that the amount of dispersion introduced by the 10X objective lens is less than that from the 63X objective lens. The TPEF intensity obtained by the 10X objective lens also shows a much sharper increase and decrease when the apex separation is away from its optimized value. Furthermore, there is no dip in the center of the intensity curve of the 10X objective lens. The different results from the 10X and 63X objective lens could be due to the different focal volumes of the two objectives. The 10X objective has a much larger focal volume than that of the 63X. The laser power is delivered into a larger sampling volume with the 10X objective. Thus it is less likely to have saturation and photobleaching with the 10X and its TPEF intensity can increase dramatically when the pulse duration is decreased. Therefore, MPM generally benefits from using a shorter pulse which can increase the peak intensity of excitation. However, MPM intensity may not increase any more if the photon flux is increased to the level of saturation. In that case, the average power of excitation can be reduce while the same intensity of MPM can still be excited due to a higher concentration of photon flux. It can thus minimize photobleach which is essential for imaging biological samples.

4.2. MPM/OCT IMAGES

With the combined MPM/OCT system, we can obtain simultaneously MPM and OCT images from the same sampling volume. Co-registered MPM/OCT images have been obtained. Fig. 6 shows the MPM and OCT images of fluorescent

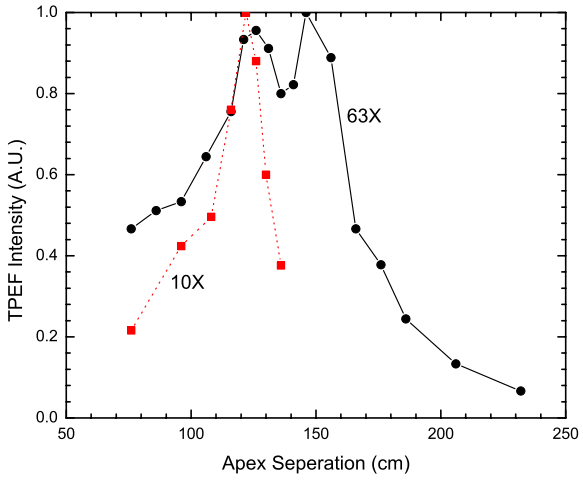

Figure 5. Intensity of TPEF with 10X and 63X objectives, respectively, under different apex separations.

beads. These fluorescent beads are of a 6 μm diameter. In both the MPM and OCT channels we can see similar images of the beads, which indicates that the MPM and OCT channels are imaging exactly the same sampling volume.

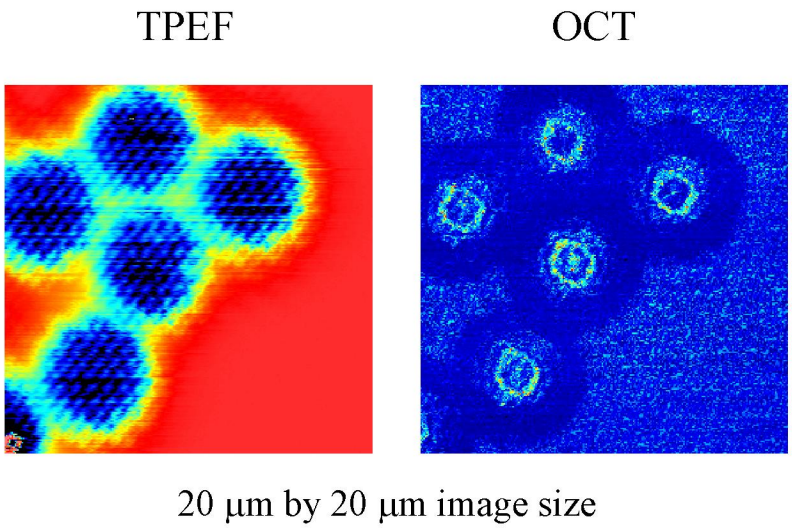

Figure 6. MPM/OCT images of fluorescent beads.

A fibroblast cluster is also imaged with the combined MPM/OCT system. The nuclei of the fibroblasts are stained with red dye and they show very bright fluorescent signal. Fig. 7 top left is the MPM image, where the nuclei are clearly seen with bright color. The top right is the corresponding OCT image from the same scanning area, where a cloud of back scattering signal is observed mostly outside of the nuclei. No SHG signal is detected in the fibroblast cluster. By overlaying the MPM and OCT images, we can see that the fluorescent and back scattering signals are from different areas of the fibroblast cluster. Therefore, the combined MPM/OCT system can show complementary information about the cells

and extracellular structure. This system will be very useful to study where the back scattering signal is from on the cellular level for the OCT technology.

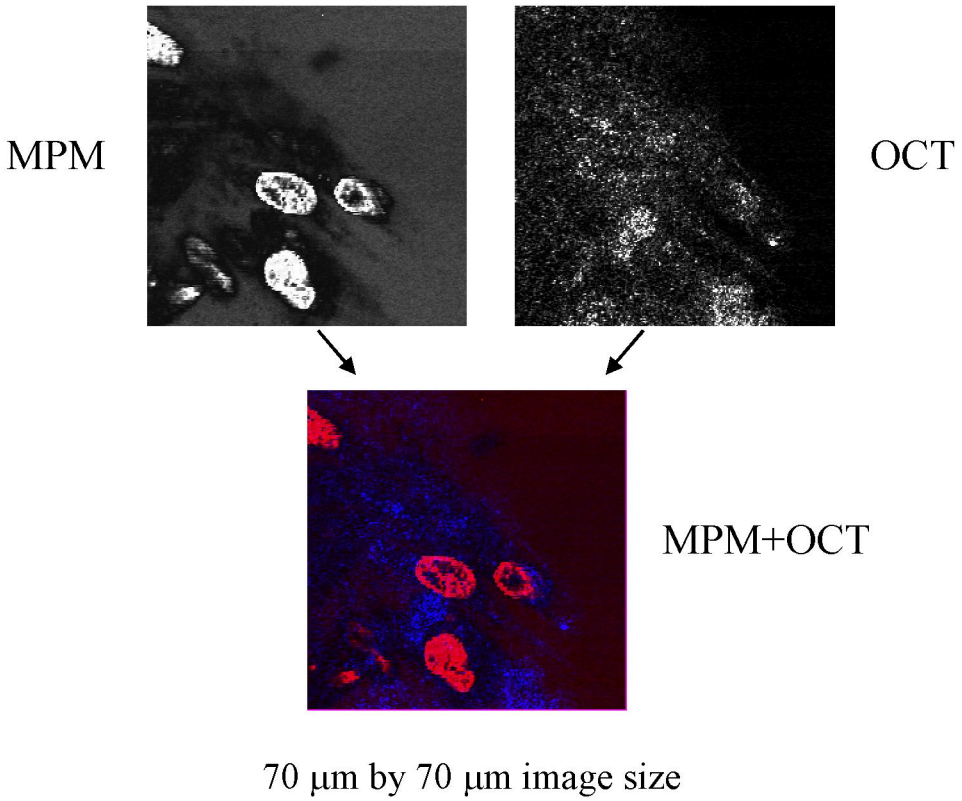

Figure 7. MPM/OCT images of fibroblast cluster.

5. CONCLUSIONS

A combined MPM/OCT system is built on the same platform. The 10 fs and 100 nm Ti:Sapphire laser provides the ultrashort pulse for MPM excitation and the broad bandwidth for high resolution OCT. The MPM and OCT images thus have similar resolution on the 1 μm order of magnitude. Co-registered images are obtained between the MPM/OCT channels. The combined MPM/OCT system can provide complementary information about cellular and extracellular structures of biological tissues simultaneously. It may also illustrate the cellular origin of OCT contrast.

ACKNOWLEDGMENTS

Shuo Tang thanks Enrico Gratton for helping on the software and Chung-Ho Sun for preparing biological samples. This research is supported by grants awarded by the National Institute of Health (RR-01192, NCI-91717).

REFERENCES

1. W. Denk, J.H. Strickler, and W.W. Webb, “Two-photon laser scanning fluorescence microscopy,” *Science*, vol. 248, no. 4951, pp. 73-76, Apr. 1990.
2. D. Huang, E.A. Swanson, C.P. Lin, J.S. Schuman, W.G. Stinson, W. Chang, M.R. Hee, T. Flotte, K. Gregory, C.A. Puliafito, and J.G. Fujimoto, “Optical Coherence Tomography,” *Science*, vol. 254, no. 5035, pp. 1178-1181, Nov. 1991.

3. A.T. Yeh, B. Kao, W.G. Jung, Z. Chen, J.S. Nelson, and B.J, Tromberg, "Imaging wound healing using optical coherence tomography and multiphoton microscopy in an *in vitro* skin-equivalent tissue model," *J. Biomed. Opt.*, vol. 9, no. 2, pp. 248-253, Mar./Apr. 2004.
4. E. Beaurepaire, L. Moreaux, F. Amblard, and J. Mertz, "Combined scanning optical coherence and two-photon-excited fluorescence microscopy," *Opt. Lett.*, vol. 24, no. 14, pp. 969-971, Jul. 1999.
5. Alberto Diaspro, *Confocal and Two-Photon Microscopy —- Foundations, Applications, and Advances*, Wiley-Liss, New York, 2002.